MODEL PREDICTION AND CLIMATOLOGY OF AEROSOL OPTICAL DEPTH (τ_{550}) AND ANGSTROM EXPONENT ($\alpha_{470\text{-}660}$) OVER THREE AEROSOL ROBOTIC NETWORK STATIONS IN SUB-SAHARAN AFRICA USING MODERATE RESOLUTION IMAGING SPECTRORADIOMETER DATA

S. B. Sharafa[1],*, R. Aliyu[2], B. B. Ibrahim[3], B. I. Tijjani[4], T. H. Darma[5], U. M. Gana[6], F. Ayedun[7] and H. T. Sulu[8]

[1,] DEPARTMENT OF PHYSICS, USMANU DANFODIYO UNIVERSITY SOKOTO, SOKOTO, SOKOTO STATE, NIGERIA
[2,] PHYSICS DEPARTMENT, KANO STATE UNIVERSITY OF SCIENCE AND TECHNOLOGY WUDIL, KANO STATE, NIGERIA
[3,] PHYSICS/ELECTRONICS UNIT, KWARA STATE POLYTECHNIC, ILORIN, KWARA STATE, NIGERIA
[4, 5, 6,] PHYSICS DEPARTMENT, BAYERO UNIVERSITY KANO, KANO, KANO STATE, NIGERIA
[7,] DEPARTMENT OF PURE AND APPLIED SCIENCE, NATIONAL OPEN UNIVERSITY OF NIGERIA, JABI, ABUJA, NIGERIA
[8,] PHYSICS/ELECTRONICS UNIT, UMARU ALI SHINKAFI POLYTECHNIC, SOKOTO, SOKOTO STATE, NIGERIA
E-mail addresses: **[1]** *sharafa.salihu@udusok.edu.ng,* **[2]** *rakiyaaliyu238@yahoo.com,*
[3] *ibb_fulani@yahoo.com,* **[4]** *idrithtijjani@gmail.com,* **[5]** *thdarma.phy@buk.edu.ng,* **[6]** *umgana@gmail.com,*
[7] *fayedun@noun.edu.ng,* **[8]** *hassansulu99@gmail.com*

ABSTRACT

The spatial and temporal variations of aerosol optical depth at 550 nm (τ_{550}) and Angstrom exponent derived from 470 and 660 nm ($\alpha_{470\text{-}660}$) over Nairobi (NAI), Skukuza (SKU) and Ilorin (ILO) Aerosol Robotic Network (AERONET) stations in sub-Saharan Africa, as recorded by Moderate Resolution Imaging Spectroradiometer (MODIS) satellites for fifteen years (2000-2015), were examined in relation to their climatologies and prediction. The MODIS measurements of τ_{550} and $\alpha_{470\text{-}660}$ from aqua (MYD04) and terra (MOD04) satellites were used in this study. Retrievals of τ_{550} for both satellites were validated with AERONET τ_{550} for the same period. The validation results showed that they compare favourably over the three stations, but MOD04 performed better than MYD04 data in NAI and ILO for τ_{550}. This shows that the τ_{550} of NAI and ILO are best captured using the MOD04 data while that of SKU is best with MYD04. It was also discovered that MODIS underestimated AERONET τ_{550} data over NAI and SKU. The most polluted station is ILO while the least polluted one is NAI. Similarly, the station with the highest concentration of absorbing aerosols is NAI and the least was observed in ILO. The aerosol climatology shows that the most polluted months in NAI, SKU and ILO are October, June and March respectively. On the other hand, February, November and March has the highest amount of scattering aerosols in the atmosphere for NAI, SKU and ILO respectively. The highest amount of absorbing aerosols was found, respectively, in the months of June, June and August. The generated time series (TS) models are all good, though a general underestimation of the parameters by the models was also observed.

Keywords: Aerosol optical depth, Angstrom exponent, MODIS, Time series, sub-Saharan Africa

1. INTRODUCTION

Atmospheric aerosols are of importance for a wide range of geophysical and environmental problems ranging from local issues to global scale. Yet, our knowledge about them is very deficient. This is to a large extent due to their complexity. Sub-Saharan

* Corresponding author, tel: +234 803 524 4296

African region is one of the biggest dust and biomass burning smoke aerosol source of the world [1]. Massive dust plumes regularly propagate from the continent to the ocean and as far as America, particularly during the wet season in the so-called Saharan air Layer [2]. These mineral particles exert a strong influence on the radiative balance and the climate. The years of rainfall deficits over West Africa are marked by anomalies in the dynamics of the monsoon system and mineral dust has kept increasing during drought years [3]. But the cause of this continuous dust increase is still unknown because it may be linked to the increase in wind intensity during dry years and/or a decrease in vegetation. A lot of studies using short time and spatially limited observed data have been conducted to characterize these particles and their impacts on the regional climate. Mineral dust particles were investigated during the SHADE campaign over the West Africa, while their radiative effects were measured in the solar spectrum by ground-based measurements [4]. The particles found in Tanré *et al*. [4] during field measurements were only dust with relatively low absorption properties.

Modeling approaches have been used by some authors [5-7] to study aerosols spatio-temporal distribution and their impacts on the climate. Despite these studies, the spatio-temporal distribution of aerosols and their radiative impacts on the climate is still an investigating topic.

The TS modeling is a useful tool in planning, operating and decision-making of climate fluctuations and is being used in data generation in so many fields [8].

Aerosol particles influence climate by modifying both the global energy balance through absorption and scattering of radiation (direct effects), and the reflectance and persistence of clouds and the development and occurrence of precipitation (indirect effects); the term "aerosol" denotes a stable, sparse suspension of microscopical or sub-microscopical solid and/or liquid particles in air. Aerosol particles contribute to numerous other climatically important processes, including fertilization of land and oceans through the deposition of nitrates, iron, and other nutrients, acidification of lakes and forests through the deposition of sulfates and nitrates, and the reduction of snow and ice albedo through the deposition of black carbon [9]. Reduction in the intensity of a direct solar beam during its propagation through the atmosphere is determined by absorption and scattering processes. These two different mechanisms contribute to extinction of light,

a term that means the loss of light in the atmosphere from a directly transmitted beam [10].

To quantify the effect of atmospheric aerosols, it is necessary to increase our understanding of the subject by studying the spatial and temporal variability of its different properties [11].

Improvements in satellite measurement capability have increased the amount of aerosol parameters retrieved from space-borne sensors.

The Moderate-resolution Imaging Spectroradiometer (MODIS) level II aerosol products from aqua- (MYD04) and terra-satellites (MOD04) are the best aerosol optical depth product suitable for near-real-time aerosol data assimilation [12]. MODIS currently provides the most extensive aerosol retrievals on a global basis, but validation is limited to a small number of ground stations [13].

To validate the aerosol retrieval parameters, ground-based measurement data are necessary. The aerosol optical properties retrieved using direct solar radiations from the sun-photometers of the Aerosol Robotic Network (AERONET) are free from surface reflectance error and cloud contamination. Therefore, AERONET dataset is widely used to evaluate the efficiency of satellite based aerosol retrieval algorithm as well as to develop new algorithm [14]. Several approaches have been proposed for the validation of MODIS aerosol retrieval algorithm for the purpose of renovating and improvement [15-18]. Kaufman *et al*. [19] proposed the first algorithm which was later modified by Levy *et al*. and Hsu *et al*. [21, 22] by proposing two different methods for aerosol retrieval.

The current study provides an attempt on τ and α climatology analysis and time series prediction using MODIS products as well as validation of MOD04/MYD04 DB collection 6 MODIS based τ with that of AERONET at 550nm over the study area for periods between years 2000 - 2015.

2. MATERIALS AND METHODS
2.1. Data Collection
Sub-Saharan Africa is the area of the African continent which lies south of the Sahara. Geographically, the demarcation line is the southern edge of the Sahara desert. The African transition zone cuts across the southern edge of the Sahara desert at the widest portion of the continent. The climate of the region is mainly characterized by two seasons; dry and raining. In addition, sub-Saharan Africa is exemplified by a warm, humid, and tropical climate. The climate is affected mostly by the urban and biomass burning, and

also the desert dust cycle which mainly originates from the Sahara and brings polluted and dry air. The distribution of AERONET stations with level 2 data used for this work is shown in Table 1.

Aerosol Robotic Network (AERONET) and Moderate Resolution Imaging Spectroradiometer (MODIS) data were used in this work. The collocated data were downloaded from the website of Multi-sensor Aerosol Products Sampling System (MAPSS) [23,24]. It provides a consistent sampling approach that enables easy and direct inter-comparison and ground-based validation of the diverse aerosol products from different satellite sensors in a uniform and consistent way [24]. The long time-series (2000-2015) of MODIS measurements of aerosol optical depth (τ_{550}) and Angstrom exponent ($\alpha_{470-660}$) was used in this study for time series (TS) modeling and forecasting over three stations in sub-Saharan African region. The study covers (NAI), Skukuza (SKU) and Ilorin (ILO). These stations are ideally placed and suitable for the TS analysis in the region.

For the long-term trend study, the stations were selected purely based on the availability of an extensive data record. Calculation of the monthly mean of the parameters (both from AERONET and MODIS) using all-point measurements was done. A monthly mean was considered valid only if there are more than five measurements for that month. To ensure a continuous time series, it was required that the data record should have at least 3 years of AERONET data measurements, with no less than eight monthly data points for each year during the 2000 to 2015 period.

The MOD04_L2/MYD04_L2 Deep Blue (DB) aerosol optical properties data from level 2 collection 6 were used in this analysis. The overall data over the entire study period were analyzed. Also analyzed are the monthly mean data of τ_{550} and $\alpha_{470-660}$ to reveal their temporal variability. The distribution patterns of anthropogenic and natural aerosols over the study region were determined.

2.2. Data Analysis

The TS model statistics and model parameters of the aerosol optical parameters for each of the study area will be derived using Expert Modeler in the SPSS package. The derived models were used to predict 2015 values for each of the parameters in each station. Evaluation of the model statistics was done for each

parameter. To evaluate the performance of the model-predicted data, precision measures (RMSE, MAPE and MAE) shall be considered. Low values of the precision measures are the standard for a good model and prediction.

2.3. Theory

The MAPSS [23] provides a consistent sampling approach that enables easy and direct inter-comparison and ground-based validation of the diverse aerosol products from different satellite sensors in a uniform and consistent way [24].

Sub-Saharan African region is influenced by various natural and anthropogenic aerosols due to its dense population and high pollution emission resulting in spatio-temporal variation [25].

The simplest method to quantify the changes in spectral τ is to estimate Ångström parameters (α and β) using Eqn. (1) [25,26,27],

$$\tau(\lambda) = \beta\lambda^{-\alpha} \tau_{abs}(\lambda) = [1 - w_o(\lambda)]\tau(\lambda) \qquad (1)$$

Aerosol optical depth (τ) is a measure of aerosol loading. Pure atmospheric conditions should be between 0.04 and 0.06 [29]. Ångström exponent (α) provides information on the aerosol size distribution while the Ångström turbidity coefficient (β) is linked to the columnar mass loading of coarse-mode aerosols.

High α and low β indicate higher quantity of fine mode aerosol concentration. The α value depends on aerosol size distribution and varies from 1 to 3 for fresh and aged smoke, and for urban aerosol particles, while it is nearly zero for coarse mode aerosols such as dust and sea salt [30]. The α can be calculated using Eqn. (2) [30,27,31]:

$$\alpha = -\frac{ln\left(\frac{\tau_1}{\tau_2}\right)}{ln\left(\frac{\lambda_1}{\lambda_2}\right)} \qquad (2)$$

Where τ_1 is the aerosol optical depth (AOD) at a reference wavelength λ_1 and τ_2 is the AOD at another wavelength λ_2.

For each wavelength, β is determined as.

$$\beta = \frac{\tau(\lambda_1)}{\lambda_1^{-\alpha}} = \frac{\tau(\lambda_2)}{\lambda_2^{-\alpha}} \qquad (3)$$

where λ must be expressed in microns (550 nm = 0.550 μ). β values of less than 0.1 are associated with a relatively clear atmosphere, and values greater than 0.2 are associated with a relatively hazy atmosphere [33].

Table 1: Aeronet stations used in the study and their coordinates

S/No	Country	Aeronet station	Longitude	Latitude	Altitude	Dry season	Region
1	Kenya	Nairobi	36°E	1°S	1650 m	Dec. to Jan., Jun. – Aug.	East Africa
2	South Africa	Skukuza	31°E	24°S	150 m	May – Sept.	Southern Africa
3	Nigeria	Ilorin	4°E	8°N	350 m	Nov. – Mar.	Western Africa

2.4. Time series (TS) analysis

Time series analysis are methods for analyzing TS data in order to extract meaningful statistics and other characteristics of the data, and to forecast future events based on known past events. The TS model will generally reflect the fact that observations close together in time will be more closely related than observations further apart. In addition, TS models will most times make use of the natural one-way ordering of time so that values for a given period will be expressed as deriving in some way from past values [8].

2.4.1. Time Series (TS) Expert Modeler

The Time Series Expert Modeler automatically identifies and estimates the best-fitting ARIMA or exponential smoothing model for one or more dependent variable series, thus eliminating the need to identify an appropriate model through trial and error.

To determine the optimum parameters of the chosen model, we use the mean absolute error (MAE), mean absolute percentage error (MAPE) and the root mean squared error (RMSE):

$$MAE = \frac{1}{n}\sum |y - \bar{y}|, \tag{4}$$

$$MAPE = \frac{1}{n}\sum \left|\frac{y - \bar{y}}{y}\right| \tag{5}$$

$$RMSE = \sqrt{\frac{1}{n}\sum (\bar{y} - y)^2} \tag{6}$$

where: n is the number of periods of time, y = actual output value and $\bar{y}$ = predicted output value.

The MAE, MAPE and the RMSE can be used together to diagnose the variation in the errors in a set of forecasts. The MAE is the average over the verification sample of the absolute values of the differences between forecast and the corresponding observation. The RMSE is the square root of the average squared values of the differences between the forecast and the corresponding observation. Those errors have the same units of measurement and depend on the units in which the data are measured [34].

3. RESULTS AND DISCUSSION

3.1. Comparisons between τ from the AERONET and MODIS

Figures 1 – 3 show the validation plots of τ_{MODIS} against $\tau_{AERONET}$ for the study area using both retrievals, including the seasonal validation. They all have good coefficient of determination (R^2 is between 0.690 – 0.935) while their respective values of standard deviation (SD) is small and fairly constant (SD between 0.130 and 0.145).

The deviation from unity of the slope of correlation plot represents systematic biases and are mainly due to aerosol model assumptions, instrument calibration or the choice of the lowest 20–50 percentile of the measurements [15, 34].

Table 2 shows the comparison of slope and R^2 values for different sites in the study area for the two satellite sensors and the combined data set. As can be observed, terra retrievals of τ_{MODIS} have a better agreement with $\tau_{AERONET}$ in NAI and ILO. Whereas, it is the aqua-retrievals that performed better at SKU. This implies that the aerosol climatology of those sites are better captured using both satellite data, as they compare well with AERONET readings.

A high R^2 (0.935) observed for ILO station using terra-MODIS sensor indicates a good agreement between MODIS and AERONET data. It also provides confidence that aerosol optical and radiative properties over study area can be analyzed using MODIS aerosol retrievals [36]. A slope of 1.083 implies an overestimation of the measured parameter by 8.3% compared to sun photometer, whereas a slope of 0.824 (observed in aqua-MODIS for SKU station) show that MODIS sensor underestimates τ with respect to AERONET by 17.6% [37].

Similarly, Table 3 shows the best retrievals of τ_{MODIS}. It could be seen that τ_{MODIS} have a better agreement with $\tau_{AERONET}$ during the dry season for NAI and ILO stations. On the other hand, the SKU data have better agreement during the raining season.

3.2. Aerosol Climatology of the stations

The mean monthly cycle of τ_{550} and $\alpha_{470 - 660}$ in the atmosphere measured between February 2000 and July 2015 for the study areas are shown in Figures 4 (a – b).
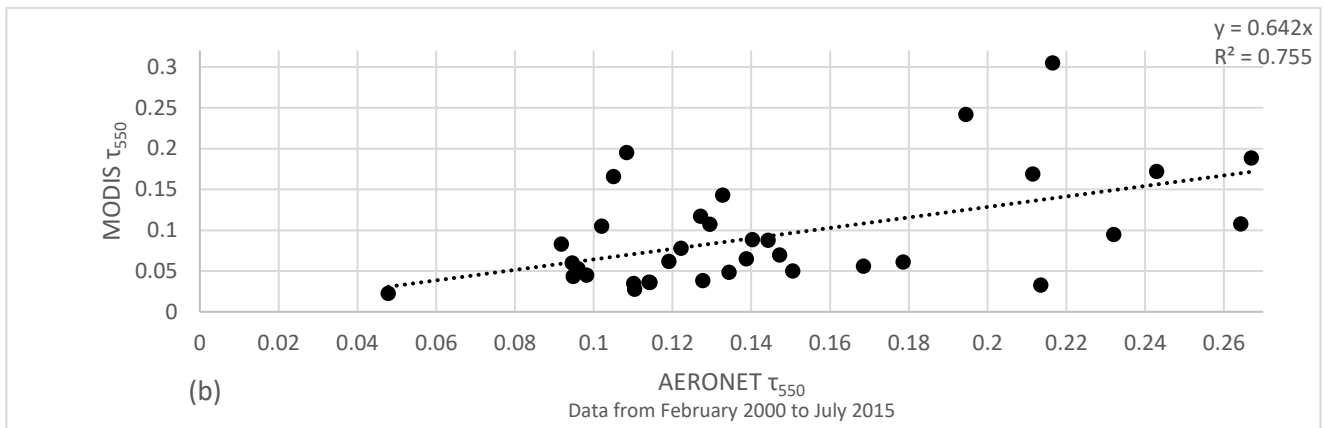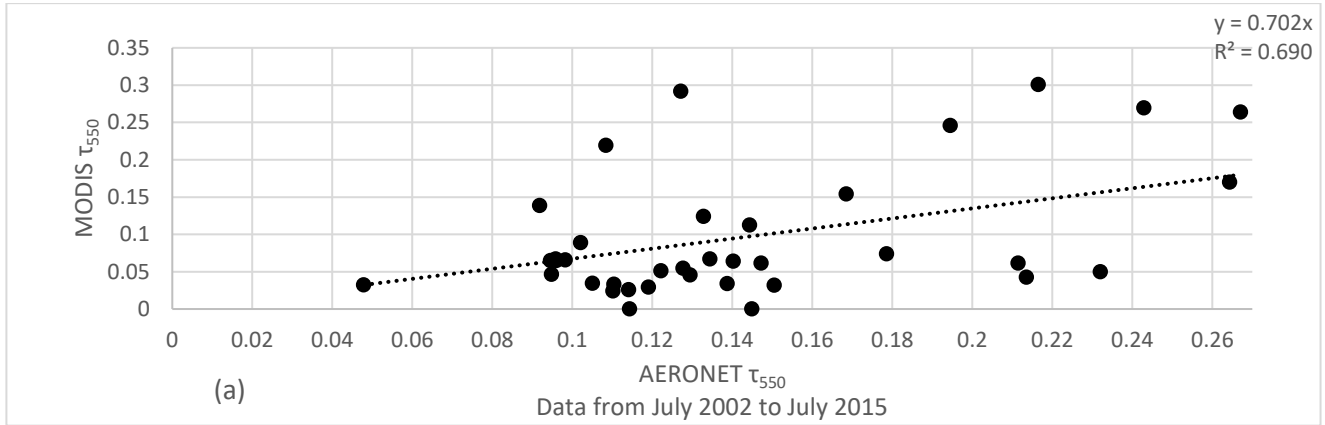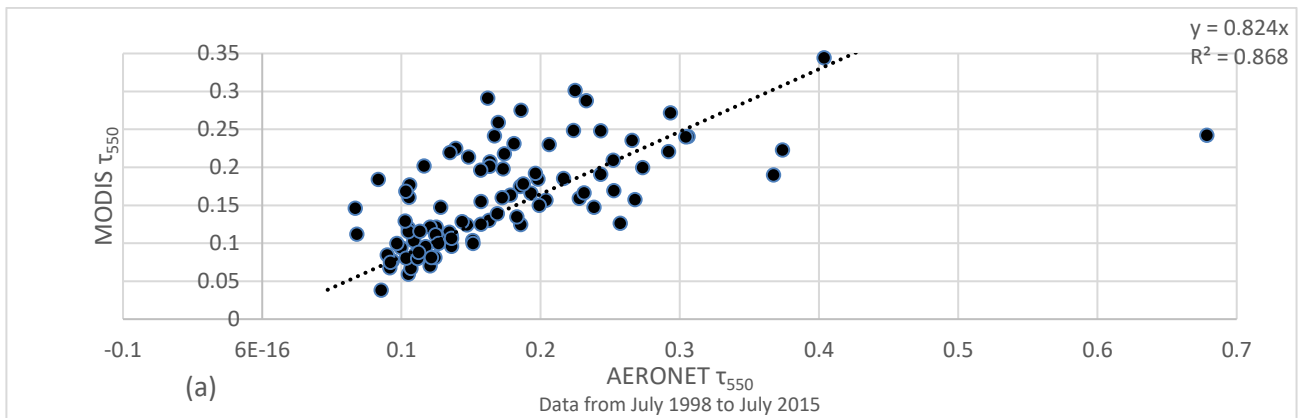
Fig. 1: Scatter plot showing the comparison of τ_{550} derived from monthly mean τ_{550} of MODIS and AERONET data for τ Nairobi using (a) aqua-MODIS satellite and (b) terra-MODIS satellite with correlation coefficient (R^2) and regression relation.
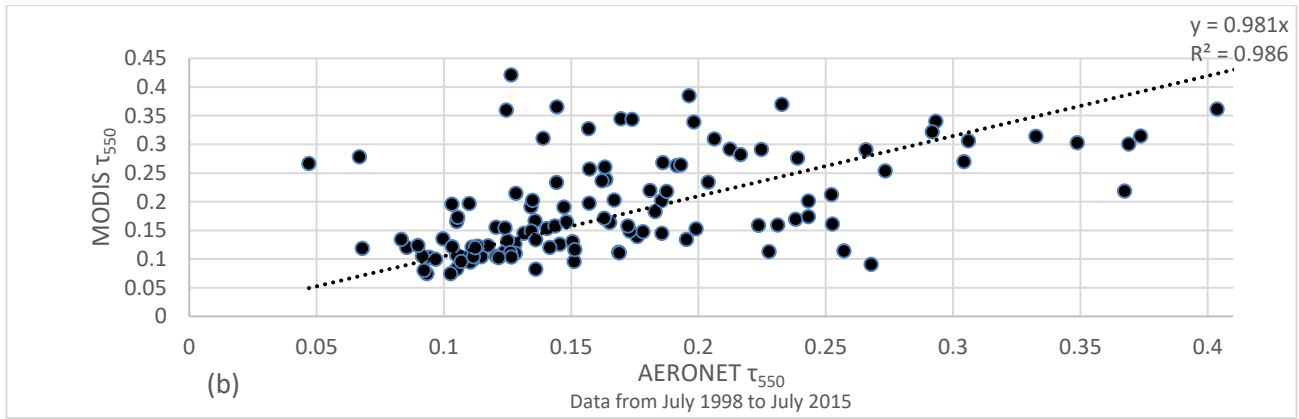
Fig. 2: Scatter plot showing the comparison of τ_{550} derived from monthly mean τ_{550} of MODIS and AERONET data for Skukuza using (a) aqua-MODIS satellite and (b) terra-MODIS satellite with correlation coefficient (R^2) and regression relation.
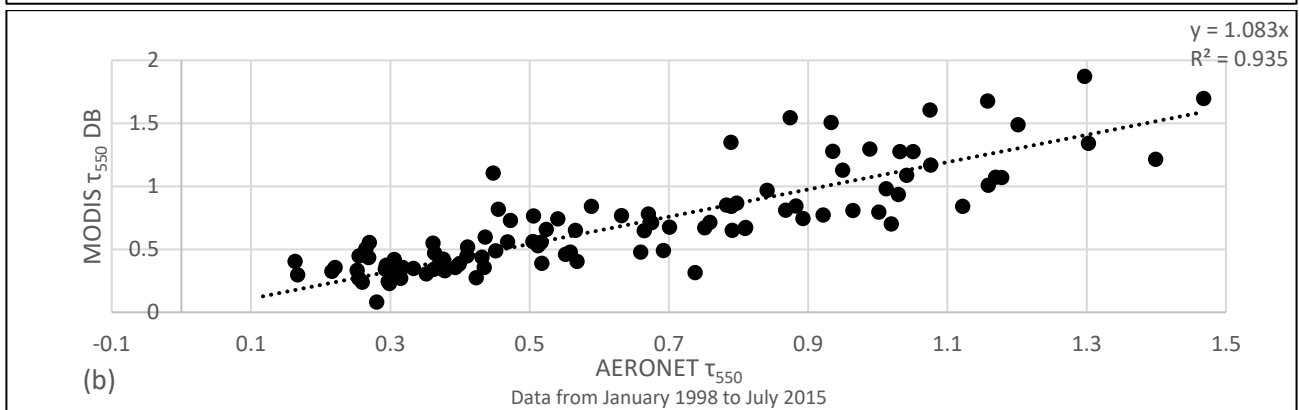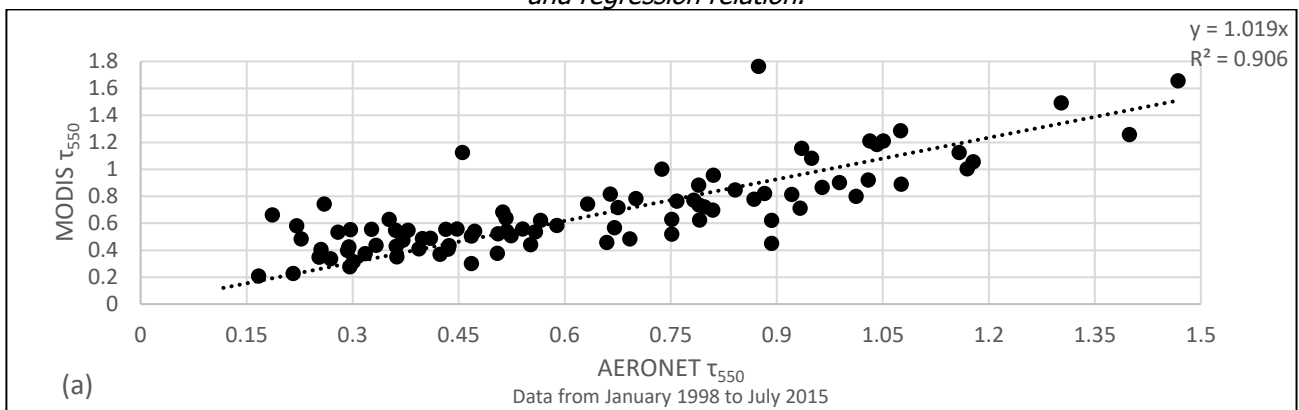

Fig. 3: Scatter plot showing the comparison of τ_{550} derived from monthly mean τ_{550} of MODIS and AERONET data for Ilorin using (a) aqua-MODIS satellite and (b) terra-MODIS satellite wit correlation coefficient (R^2) and regression relation.

Table 2: The Slope and coefficient of determination (R^2) of the regression analysis of the scatter plots of τ_{MODIS} against $\tau_{AERONET}$

Case	Aqua-MODIS		Terra-MODIS	
	Slope	R^2	Slope	R^2
Nairobi	0.702	0.690	0.642	0.755
Skukuza	0.824	0.868	0.981	0.786
Ilorin	1.029	0.930	1.083	0.935

Table 3: The Slope and R² for the Different Validation Cases at 550 nm during each season across the study area

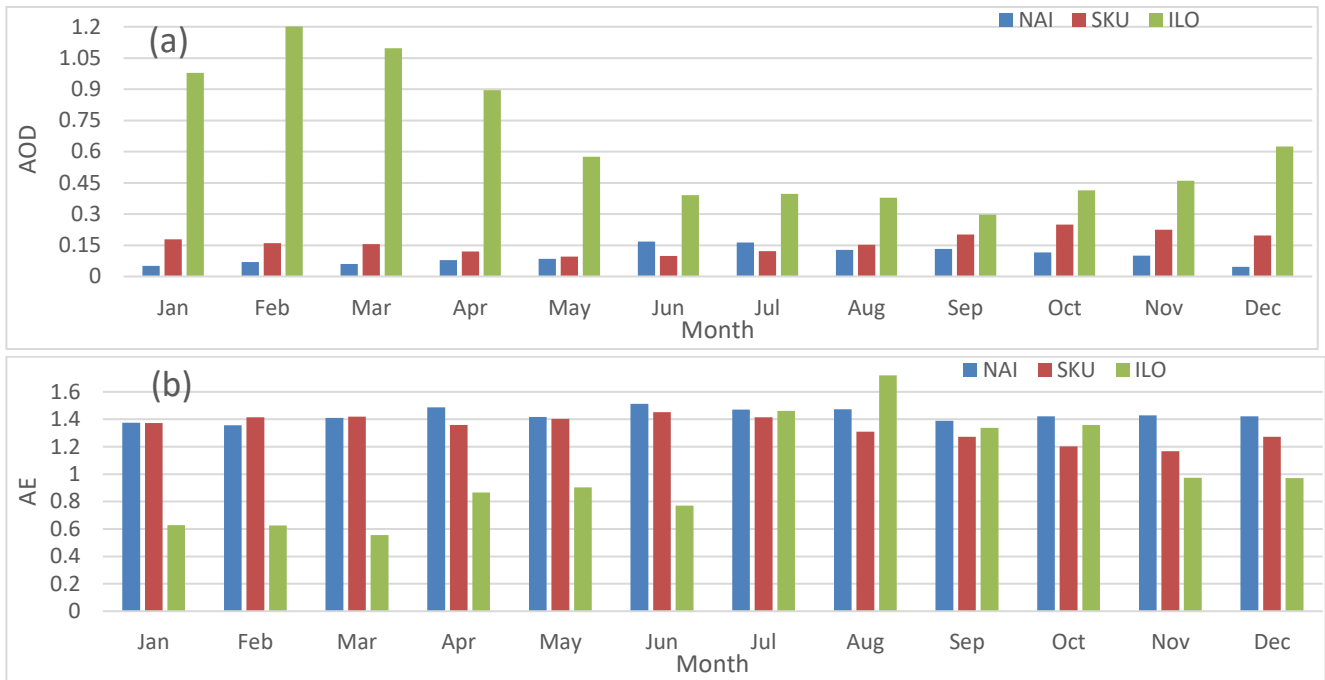| Case	Aqua-MODIS		Terra-MODIS	
	Slope	R^2	Slope	R^2
Nairobi	0.499	0.878	0.703	0.751
Skukuza	0.818	0.774	0.828	0.948
Ilorin	1.072	0.951	1.134	0.876

Fig. 4: Monthly cycle of mean (a) τ and (b) α in Nairobi, Skukuza and Ilorin stations ngth

It is clear from the Figure 4 (a) that the monthly mean τ values in NAI present low values with the highest (~0.17) being in July and the lowest (~0.05) being in December. This station shows trend that are traits of all low aerosol loading regions. Nevertheless, the atmosphere here is a polluted one (i.e., τ > 0.05). From the same figure, the values for SKU were higher. The highest value in this station is ~0.25 and was observed in October while 0.096 observed in May was the lowest value. Lastly, the highest value in ILO (1.20) was observed in February while the lowest was 0.30 and was observed in September.

The three stations has a polluted atmosphere since their values of the mean monthly τ is greater than 0.05. The cleanest month in NAI, SKU and ILO stations respectively is December, May and September. August. τ values start decreasing in wet season (April to August) and increases significantly during dry (November – March). This cycle starts in November, when aerosol concentration begins to build up in the atmosphere; it increases continuously, depicting its peaks in March (a transition month). The month with

the lowest mean monthly τ is August, and with a high α₄₇₀₋₆₆₀ values indicate the presence of aerosol types other than dust. It may be any of maritime, biomass burning, continental origin or their combination. These patterns of monthly cycle of τ (increase after wet season and decrease after dry season) remain consistent during the 16 years of study.

The observed seasonal pattern can be associated with fairly moderate concentrations of coarse mode aerosol during dry. Similar conclusion was drawn by Kaskaoutis *et al*. [38], and is supported by our observed low α₄₇₀₋₆₆₀ values in ILO station. The transport of dust aerosol from the Sahara to the sub-Saharan African region by northeasterly dry wind during dry has been reported by Balarabe *et al*. [39]. The seasonal dependence of τ has resulted in the corresponding seasonal feature of α as seen in Figure 4 (b). The lowest value (1.357) of mean α₄₇₀₋₆₆₀ observed in February at NAI station shows a slight reduction in the amount of fine mode aerosols in the atmosphere around the station. The lowest value (1.168) in SKU station was observed November, and

is also as a result of reduction in quantity of fine mode aerosols in the area whereas the lowest value (0.555) in ILO station observed in March is a signature of mineral dust [40]. The value of mean $\alpha_{470-660}$ was observed to increase during rainy season as a result of which significant amount of the larger particles were washed down from the atmosphere. This natural phenomenon causes the $\alpha_{470-660}$ to become larger.

The three stations can be said to have poor air quality all year round for having the minimum monthly $\tau_{550} >$ 0.05. According to Toledano *et al.* [41], the average τ values under clean background condition should be less than 0.05.

3.3. Time series analysis and prediction
3.3.1. τ_{550} analysis and prediction

The TS model statistics of the τ_{550} for each of the AERONET stations in the sub-Saharan African region are given in tables 4 - 6. It is obvious from the tables that not all the models are statistically significant.

From the Table 4, the model obtained in Nairobi is simple seasonal exponential smoothing. This shows that the τ_{550} in this station did not increase significantly over the years and its seasonal effect is constant for these years. The values of the stationary R^2 (0.692) and R^2 (0.275) show that the model is good, but statistically insignificant. The low values of RMSE (0.064), MAPE (66.467), MAE (0.047) and a negative

Normalized BIC (-5.425) shows that the model is good. Also, from the values of the significance of the model parameters, it can be seen that the level parameter is statistically significant while the season parameter is not. The season parameter indicates that the τ_{550} in this station is seasonal in nature.

Figure 5 shows plot of τ_{550} measured and predicted using the model statistics in Table 4, for Nairobi station. For the validation of τ_{550} in Figure 5, MAE was 0.0497; MAPE was 0.5006 and RMSE was 0.0639. The plot shows that the model can estimate the parameter well.

From the Table 5, the model obtained for τ_{550} in Skukuza is simple seasonal exponential smoothing. This shows that the τ_{550} in this station did not increase significantly over the years and its seasonal effect is constant for these years. The values of the stationary R^2 (0.696) and R^2 (0.542) show that the model is good, but statistically insignificant. The low values of RMSE (0.044), MAPE (22.938), MAE (0.033) and a negative Normalized BIC (-6.186) shows that the model is good. Also, from the values of the significance of the model parameters, it can be seen that the level parameter is statistically significant while the season parameter is not. The season parameter indicates that the τ_{550} in this station is seasonal in nature.

Table 4: Model summary of τ_{550} at Nairobi station (Kenya)

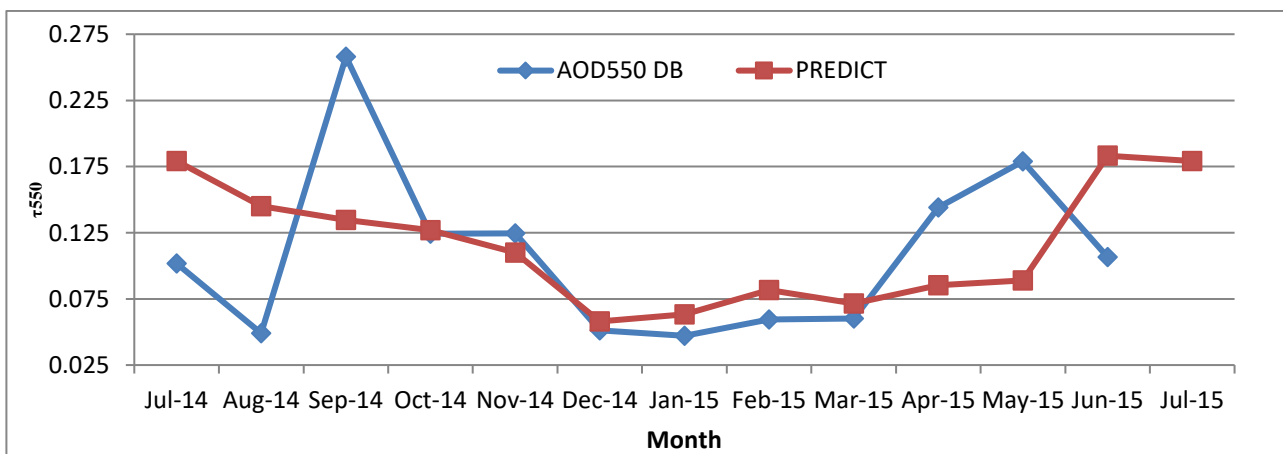| Model				Simple Seasonal		
Stationary R^2	R^2	RMSE	MAPE	MAE	Normalized BIC	Sig.
0.692	0.275	0.064	66.467	0.047	-5.425	0.367
Exponential smoothing model parameters						
No Transformation		Estimates			Sig.	
Alpha (Level)		0.099			0.027	
Delta (Season)		1.140E-005			1.000	

Fig. 5: The plots of measured and predicted τ_{550} for Nairobi station using time series analysis

Table 5: Model summary of τ_{550} at Skukuza (South Africa)

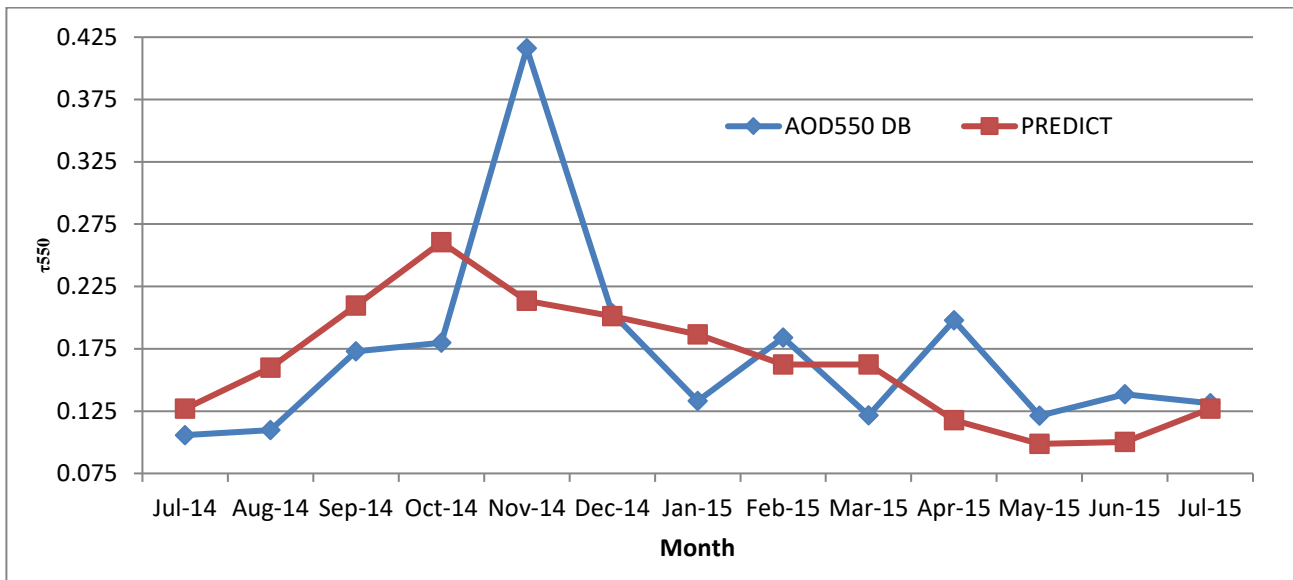| Model				Simple Seasonal		
Stationary R^2	R^2	RMSE	MAPE	MAE	Normalized BIC	Sig.
0.696	0.542	0.044	22.938	0.033	-6.186	0.256
Exponential smoothing model parameters						
No Transformation		Estimates			Sig.	
Alpha (Level)		0.100			0.018	
Delta (Season)		1.633E-007			*1.000*	

Fig. 6: The plots of measured and predicted τ_{550} for Skukuza station using time series analysis

Table 6: Model summary of τ_{550} at Ilorin station (Nigeria)

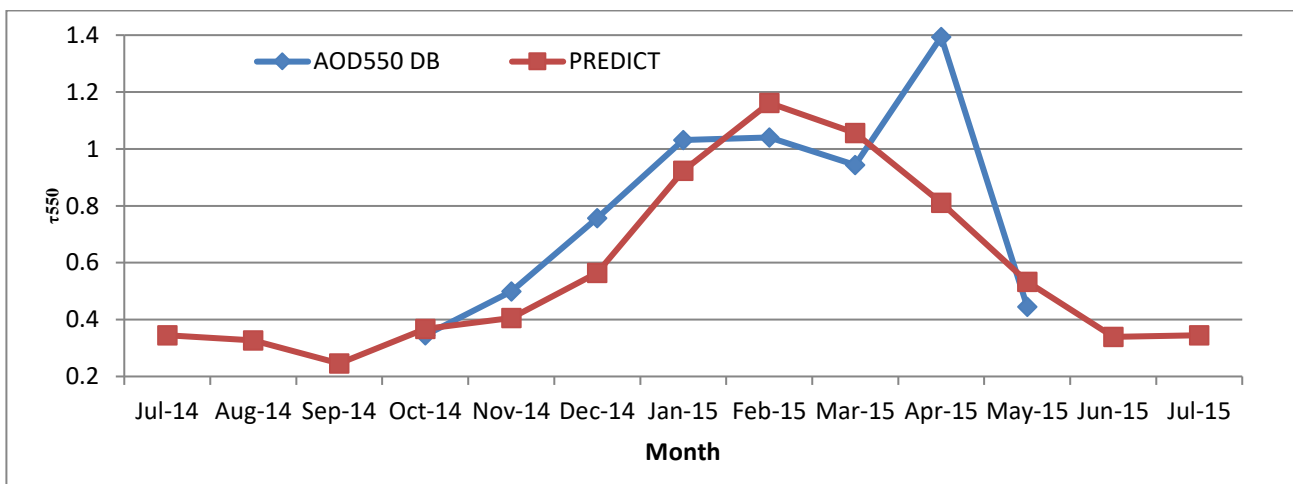| *Model*				Simple Seasonal		
Stationary R^2	R^2	RMSE	MAPE	MAE	Normalized BIC	Sig.
0.773	0.637	0.229	27.478	0.170	-2.879	0.093
Exponential smoothing model parameters						
No Transformation		Estimates			Sig.	
Alpha (Level)		0.100			0.041	
Delta (Season)		3.035E-006			*1.000*	

Fig. 7: The plots of measured and predicted τ_{550} for Ilorin station using time series analysis

Figure 6 shows plot of τ_{550} measured and predicted using the model statistics in Table 5, for Skukuza station. For the validation of τ_{550} in Figure 6, MAE was 0.0540; MAPE was 0.2942 and RMSE was 0.0737. The plot shows that the model can estimate the parameter well.

From the Table 6, the model obtained for τ_{550} in Ilorin is simple seasonal exponential smoothing. This shows that the τ_{550} in this station did not increase significantly over the years and its seasonal effect is constant for these years. The values of the stationary R^2 (0.773) and R^2 (0.637) show that the model is good, but statistically insignificant. The low values of RMSE (0.229), MAPE (27.478), MAE (0.170) and a negative Normalized BIC (-2.879) shows that the model is good. Also, from the values of the significance of the model parameters, it can be seen that the level parameter is statistically significant while the season parameter is not. The season parameter indicates that the aerosol loading in this station is seasonal in nature.

Figure 7 shows plot of τ_{550} measured and predicted using the model statistics in Table 6, for Ilorin station. For the validation of τ_{550} in Figure 7, MAE was 0.1652; MAPE was 0.1829 and RMSE was 0.2326. The plot shows that the model can estimate the parameter well.

3.3.2. $\alpha_{470-660}$ *analysis and prediction*

The TS model statistics of the $\alpha_{470-660}$ for each of the AERONET stations in the sub-Saharan African region are given in Tables 7 - 9. It is obvious from the tables that not all the models are statistically significant.

From the Table 7, the model obtained for the $\alpha_{470-660}$ at Nairobi is also simple seasonal exponential smoothing. This shows that the $\alpha_{470-660}$ in this station did not increase over the years and its seasonal effect is constant for these years. The values of the stationary R^2 (0.766) and R^2 (0.100) show that the model is good, but statistically insignificant. The low values of RMSE (0.141), MAPE (7.738), MAE (0.102) and a negative Normalized BIC (-3.858) shows that the model is good. Also, from the values of the significance of the model parameters, it can be seen that the level parameter is statistically significant while the season parameter is not. The season parameter in this model shows that the trend is seasonal, even if not significant.

Figure 8 shows plot of $\alpha_{470-660}$ measured and predicted using the model statistics in Table 7, for Nairobi station. For the validation of $\alpha_{470-660}$ in Figure 8, MAE was 0.1248; MAPE was 0.0905 and RMSE was 0.1547. The plot shows that the model can estimate the parameter well.

From the Table 8, the model obtained for $\alpha_{470-660}$ in Skukuza is simple seasonal exponential smoothing. This shows that the $\alpha_{470-660}$ in this station did not increase significantly over the years and its seasonal effect is constant for these years. The values of the stationary R^2 (0.620) and R^2 (0.401) show that the model is good, but statistically insignificant. The low values of RMSE (0.117), MAPE (6.872), MAE (0.090) and a negative Normalized BIC (-4.215) shows that the model is good. Also, from the values of the significance of the model parameters, it can be seen that the level parameter is statistically significant while the season parameter is not. The season parameter indicates that the $\alpha_{470-660}$ in this station is seasonal in nature.

Figure 9 shows plot of $\alpha_{470-660}$ measured and predicted using the model statistics in Table 8, for Skukuza station. For the validation of $\alpha_{470-660}$ in Figure 9, MAE was 0.1018; MAPE was 0.0841 and RMSE was 0.1266. The plot shows that the model can estimate the parameter well.

From the Table 9, the model obtained for the $\alpha_{470-660}$ at Ilorin is simple seasonal exponential smoothing. This shows that the $\alpha_{470-660}$ in this station did not increase over the years and its seasonal effect is constant for these years. The values of the stationary R^2 (0.719) and R^2 (0.502) show that the model is good, and also statistically significant. The low values of RMSE (0.308), MAPE (51.045), MAE (0.228) and a negative Normalized BIC (-2.287) shows that the model is good. Also, from the values of the significance of the model parameters, it can be seen that the level parameter is statistically significant while the season parameter is not. The season parameter in this model shows that the trend is seasonal, even if not significant.

Figure 10 shows plot of $\alpha_{470-660}$ measured and predicted using the model statistics in Table 9, for Ilorin station. For the validation of $\alpha_{470-660}$ in Figure 10, MAE was 0.088; MAPE was 0.2106 and RMSE was 0.1108. The plot shows that the model can estimate the parameter well.

Table 7: Model summary of $\alpha_{470-660}$ at Nairobi station (Kenya)

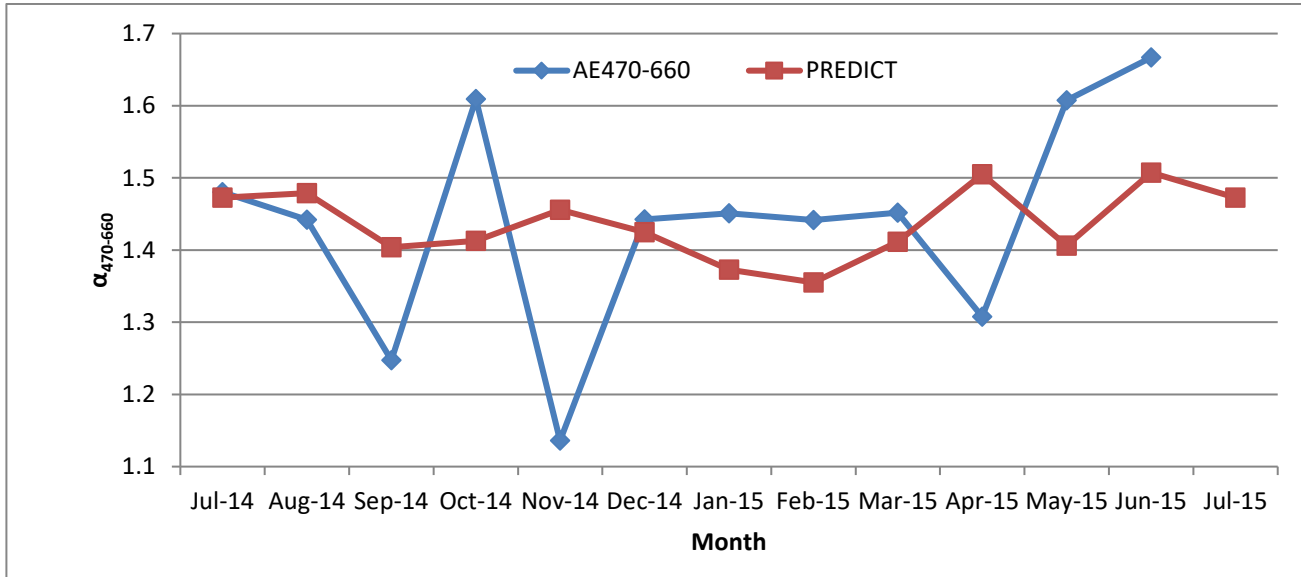| Model				Simple Seasonal		
Stationary R^2	R^2	RMSE	MAPE	MAE	Normalized BIC	Sig.
0.766	0.100	0.141	7.738	0.102	-3.858	0.084
Exponential smoothing model parameters						
No Transformation			Estimates		Sig.	
Alpha (Level)			0.100		0.010	
Delta (Season)			9.144E-006		*1.000*	

Fig. 8: The plots of measured and predicted $\alpha_{470-660}$ for Nairobi station using time series analysis

Table 8: Model summary of $\alpha_{470-660}$ at Skukuza station (South Africa)

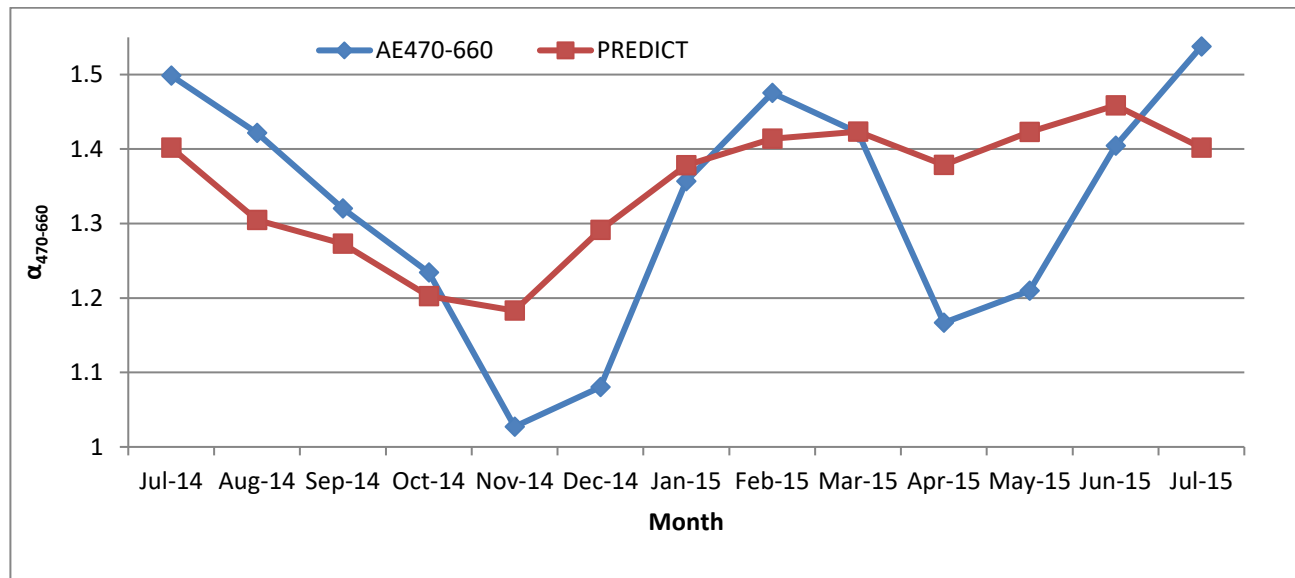| Model				Simple Seasonal		
Stationary R^2	R^2	RMSE	MAPE	MAE	Normalized BIC	Sig.
0.620	0.401	0.117	6.872	0.090	-4.215	0.596
Exponential smoothing model parameters						
No Transformation			Estimates		Sig.	
Alpha (Level)			0.200		0.000	
Delta (Season)			2.704E-006		1.000	

Fig. 9: The plots of measured and predicted $\alpha_{470-660}$ for Skukuza station using time series analysis

Table 9: Model summary of $\alpha_{470\text{-}660}$ at Ilorin station (Nigeria)

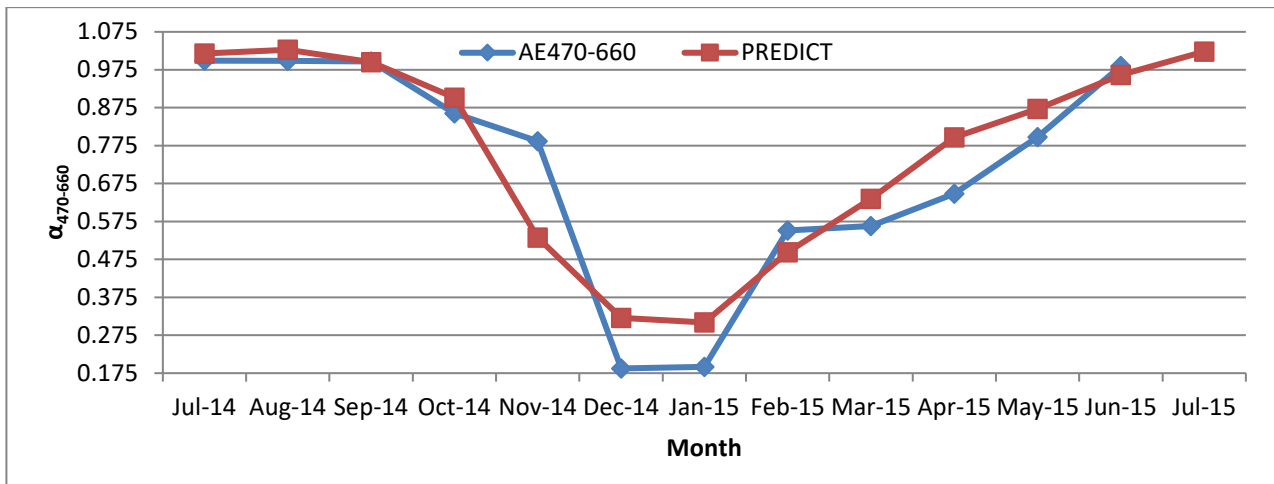| Model				Simple Seasonal		
Stationary R^2	R^2	RMSE	MAPE	MAE	Normalized BIC	Sig.
0.719	0.502	0.308	51.045	0.228	-2.287	0.000
Exponential smoothing model parameters						
No Transformation			Estimates		Sig.	
Alpha (Level)			0.100		0.003	
Delta (Season)			5.332E-006		1.000	

Fig. 10: The plots of measured and predicted $\alpha_{470\text{-}660}$ for Ilorin station using time series analysis

4. CONCLUSIONS

In this study, long-term (2000 to 2015) MODIS τ_{550} and $\alpha_{470\text{-}660}$ observed at AERONET stations in three sub-Saharan African countries have been analyzed. Analysis of their variability and TS modeling and prediction was done. The 15 years measurement show obvious variation in the parameters considered. Aerosol optical properties in the three stations display significant day-to-day variations. Monthly average values of τ_{550} range from very low ($\tau_{550} < 0.047$) to very high ($\tau_{550} > 1.202$) conditions with NAI station having the least ($0.047 \leq \tau_{550} \leq 0.168$), followed by SKU station ($0.096 \leq \tau_{550} \leq 0.250$) and ILO station ($0.297 \leq \tau_{550} \leq 1.202$). Ångström exponent ($\alpha_{470\text{-}660}$) values indicated a wide range of particle sizes (0.555 – 1.722); absorbing aerosols were the most predominant in NAI and SKU stations (with $\alpha_{470\text{-}660}$ values between 1.168 and 1.514). On the other hand, ILO station was characterized by scattering aerosols because more than 90 % of the values of $\alpha_{470\text{-}660}$ were less than unity.

TS models derived from the Expert modeler for each parameter, from the different AERONET stations, show that all the three models for the τ_{550} were Exponential Smoothing models. All of them are Simple Seasonal models. Similar models were obtained for $\alpha_{470\text{-}660}$ in the three stations too. The results from the validation of the predicted data with the data left out of the modeling stage show a very good agreement because the error parameters (MAE, MAPE and RMSE) gave low values. This indicated that the Expert Modeler in the SPSS package can be used successfully for the prediction of τ_{550} and $\alpha_{470\text{-}660}$ in the sub-Saharan African region.

Subsequent research can focus on a long term forecast of the parameters for the stations explored here, and other stations that may have long term data that are suitable for such analysis.

Therefore, it can be recommended that Aluminium silicates (mullite) which is also readily available be incorporated in the investment slurry instead of silica sand and the properties of castings could be compared with those of the present investigation.

5. REFERENCES

[1]. S. Woodward, "Modeling the atmospheric life cycle and radiative impact of mineral dust in the Hadley Centre climate model," *J. Geophys. Res.*, vol. 106, no. D16, pp. 18155–18166, 2001.

[2]. M. Drame, G. S. Jenkins, M. Camara, and M. Robjhon, "Observations and simulation of a Saharan air layer event with a midtropospheric dust layer at Dakar, Senegal, 6-7 July 2010," *J. Geophys. Res. Atmos.*, vol. 116, no. 21, pp. 6–7, 2011.

[3]. J. M. Prospero, P. Ginoux, O. Torres, S. E. Nicholson, and T. E. Gill, "Environmental characterization of global sources of atmospheric soil dust identified with the NIMBUS 7 Total Ozone Mapping Spectrometer (TOMS) absorbing aerosol product," *Rev. Geophys.*, vol. 40, no. 1, p. 1002, 2002.

[4]. D. Tanré *et al.*, "Measurement and modeling of the Saharan dust radiative impact: Overview of the Saharan Dust Experiment (SHADE)," *J. Geophys. Res.*, vol. 108, no. D18, p. 8574, 2003.

[5]. G. Myhre, C. R. Hoyle, T. F. Berglen, B. T. Johnson, and J. M. Haywood, "Modeling of the solar radiative impact of biomass burning aerosols during the Dust and Biomass-burning Experiment (DABEX)," *J. Geophys. Res. Atmos.*, vol. 113, no. 23, pp. 1–10, 2008.

[6]. G. Myhre *et al.*, "Modelled radiative forcing of the direct aerosol effect with multi-observation evaluation," *Atmos. Chem. Phys.*, vol. 9, no. 4, pp. 1365–1392, 2009.

[7]. M. Camara, G. Jenkins, and A. Konare, "Impacts of dust on West African climate during 2005 and 2006," *Atmos. Chem. Phys. Discuss.*, vol. 10, pp. 3053–3086, 2010.

[8]. K. Soni, K. S. Parmar, and S. Kapoor, "Time series model prediction and trend variability of aerosol optical depth over coal mines in India," *Environ. Sci. Pollut. Res.*, vol. 22, no. 5, pp. 3652–3671, 2015.

[9]. S. J. Ghan and S. E. Schwartz, "Aerosol properties and processes: A Path from Field and Laboratory Measurements to Global Climate Models, A report by The U.S. Department of Energy strategy for improving the treatment of aerosol properties and processes in global climate models involves ," 2007.

[10]. S. Mogo, V. E. Cachorro, A. de Frutosa, and A. Rodrigues, "Absorption om exponents of aerosols and light absorbing carbon a , central Portugal," *J. Environ. Monit.*, vol. 14, pp. 3174–3181, 2012.

[11]. M. J. Granados-Munoz, D. Pozo-Vazquez, J. L. Guerrero-Rascado, and L. Alados-Arboledas, "Study of aerosol optical properties over the Iberian Peninsula based on a 9-year MODIS Dataset," in *Proceedings of the Global Conference on Global Warming 2011, 11 - 14 July,Lisbon, Portugal*, 2011, pp. 1–10.

[12]. J. Zhang and J. S. Reid, "MODIS aerosol product analysis for data assimilation: Assessment of over-ocean level 2 aerosol optical thickness retrievals," *J. Geophys. Res. Atmos.*, vol. 111, no. 22, pp. 1–17, 2006.

[13]. Z. Li *et al.*, "Validation and understanding of Moderate Resolution Imaging Spectroradiometer aerosol products (C5) using ground-based measurements from the handheld Sun photometer network in China," *J. Geophys. Res. Atmos.*, vol. 112, no. D22S07, pp. 1–16, 2007.

[14]. A. Misra, A. Jayaraman, and D. Ganguly, "Validation of Version 5 . 1 MODIS Aerosol Optical Depth (Deep Blue Algorithm and Dark Target Approach) over a Semi-Arid Location in Western India," *Aerosol Air Qual. Res.*, vol. 15, pp. 252–262, 2015.

[15]. D. A. Chu, Y. J. Kaufman, C. Ichoku, L. A. Remer, D. Tanré, and B. N. Holben, "Validation of MODIS aerosol optical depth retrieval over land," *Geophys. Res. Lett.*, vol. 29, no. 12, pp. 1–4, 2002.

[16]. C. Ichoku *et al.*, "A spatio-temporal approach for global validation and analysis of MODIS aerosol products," *Geophys. Res. Lett.*, vol. 29, no. 12, pp. 1–4, 2002.

[17]. R. C. Levy *et al.*, "Evaluation of the MODIS Aerosol Retrievals over Ocean and Land during CLAMS," *J. Atmos. Sci.*, vol. 62, pp. 974–992, 2005.

[18]. R. C. Levy *et al.*, "Global evaluation of the Collection 5 MODIS dark-target aerosol products over land," *Atmos. Chem. Phys.*, vol. 10, no. 21, pp. 10399–10420, 2010.

[19]. Y. J. Kaufman, D. Tanré, L. A. Remer, E. F. Vermote, A. Chu, and B. N. Holben, "Operational remote sensing of tropospheric aerosol over land from EOS moderate resolution imaging spectroradiometer," *J. Geophys. Res.*, vol. 102, no. D14, p. 17051, 1997.

[20]. R. C. Levy, L. A. Remer, S. Mattoo, E. F. Vermote, and Y. J. Kaufman, "Second-generation operational algorithm: Retrieval of aerosol properties over land from inversion of Moderate Resolution Imaging Spectroradiometer spectral reflectance," *J. Geophys. Res. Atmos.*, vol. 112, no. 13, pp. 1–21, 2007.

[21]. N. C. Hsu *et al.*, "Aerosol Properties over Bright-Reflecting Source Regions," *IEEE Trans. Geosci. Remote Sens.*, vol. 42, no. 3, p. 23, 2004.

[22]. R. C. Levy, L. Remer, S. Mattoo, E. Vermote, and Y. J. Kaufman, "Second-generation algorithm for retrieving aerosol properties over land from

MODIS spectral reflectance," *J. Geophys. Res*, vol. 112, no. D13, p. D13, 2007.

[23]. M. A. P. S. S. (MAPSS), "(http://giovanni.gsfc.nasa.gov/mapss/)."

[24]. M. Petrenko, C. Ichoku, and G. Leptoukh, "Multi-sensor Aerosol Products Sampling System (MAPSS)," *Atmos. Meas. Tech*, vol. 5, pp. 913–926, 2012.

[25]. S. Tiwari, A. K. Srivastava, A. K. Singh, and S. Singh, "Identification of aerosol types over Indo-Gangetic Basin: implications to optical properties and associated radiative forcing," *Environ. Sci. Pollut. Res.*, vol. 22, no. 16, pp. 12246–12260, 2015.

[26]. K. F. Boersma and J. P. de Vroom, "Validation of MODIS aerosol observations over the Netherlands with GLOBE student measurements," *J. Geophys. Res. Atmos.*, vol. 111, no. 20, 2006.

[27]. K. R. Kumar *et al.*, "Long-term (2003-2013) climatological trends and variations in aerosol optical parameters retrieved from MODIS over three stations in South Africa," *Atmos. Environ.*, vol. 95, pp. 400–408, 2014.

[28]. B. I. Tijjani, A. Aliyu, and F. Sha, "The Effect of Relative Humidity on Continental Average Aerosols," *Open J. Appl. Sci.*, vol. 4, no. June, pp. 399–423, 2014.

[29]. F. Tan, H. S. Lim, K. Abdullah, T. L. Yoon, and B. Holben, "AERONET data – based determination of aerosol types," *Atmos. Pollut. Res.*, vol. 6, pp. 682–695, 2015.

[30]. T. F. Eck *et al.*, "Wavelength dependence of the optical depth of biomass burning, urban, and desert dust aerosols," *J. Geophys. Res. D Atmos.*, vol. 104, no. 1, p. 31,333-31,349, 1999.

[31]. B. I. Tijjani and D. O. Akpootu, "The effect of Soot and Water Solubles in Radiative Forcing of Urban Aerosols," *Int. J. Res. Rev. Pharm. Appl. Sci.*, vol. 2, no. 6, pp. 1128–1143, 2012.

[32]. L. He, L. Wang, A. Lin, M. Zhang, M. Bilal, and M. Tao, "Aerosol Optical Properties and Associated Direct Radiative Forcing over the Yangtze River

Basin during 2001–2015," *Remote Sens.*, vol. 9, no. 7, p. 746, 2017.

[33]. D. O. Akpootu and M. Momoh, "The Ångströ;m Exponent and Turbidity of Soot Component in the Radiative Forcing of Urban Aerosols," *Niger. J. Basic Appl. Sci.*, vol. 21, no. 1, pp. 70–78, 2013.

[34]. M. Murat, I. Malinowska, H. Hoffmann, and P. Baranowski, "Statistical modelling of agrometeorological time series by exponential smoothing," *Int. AGROPHYSICS*, vol. 30, pp. 57–65, 2016.

[35]. L. A. Remer *et al.*, "The MODIS Aerosol Algorithm, Products, and Validation," *J. Atmos. Sci.*, vol. 62, no. 4, pp. 947–973, 2005.

[36]. L. He, L. Wang, A. Lin, M. Zhang, M. Bilal, and M. Tao, "Aerosol Optical Properties and Associated Direct Radiative Forcing over the Yangtze River Basin during 2001 – 2015," *Remote Sens.*, vol. 9, no. 746, pp. 1–23, 2017.

[37]. H. Bibi, K. Alam∗, and S. Bibi, "In-depth discrimination of aerosol types using multiple clustering techniques over four locations in Indo-Gangetic plains," *Atmos. Res.*, vol. 181, no. 4, pp. 106–114, 2016.

[38]. D. G. Kaskaoutis, H. D. Kambezidis, N. Hatzianastassiou, P. G. Kosmopoulos, and K. V. S. Badarinath, "Aerosol climatology : dependence of the Angstrom exponent on wavelength over four AERONET sites," *Atmos. Chem. Phys. Discuss.*, pp. 7347–7397, 2007.

[39]. M. Balarabe, K. Abdullah, and M. Nawawi, "Long-Term Trend and Seasonal Variability of Horizontal Visibility in Nigerian Troposphere," *Atmosphere (Basel).*, vol. 6, pp. 1462–1486, 2015.

[40] K. Ogunjobi, V. Ajayi, I. Balogun, J. Omotosho, and Z. He, "The synoptic and optical characteristics of the harmattan dust spells over Nigeria," *Theor. Appl. Climatol.*, vol. 93, no. 1–2, pp. 91–105, 2008.

[41] C. Toledano *et al.*, "Aerosol optical depth and Angstrom exponent climatology at El Arenosillo AERONET site (Huelva , Spain)," *Q. J. R. Meteorol. Soc.*, vol. 133, pp. 795–807, 2007.